PERGAMON

Water Research 37 (2003) 3954–3966

WATER RESEARCH

www.elsevier.com/locate/watres

Removal of lead from contaminated water bodies using sea nodule as an adsorbent

S. Bhattacharjee*, S. Chakrabarty, S. Maity, S. Kar, P. Thakur, G. Bhattacharyya

Analytical Chemistry Division, National Metallurgical Laboratory, C.S.I.R, Jamshedpur 831007, India

Received 17 May 2002; received in revised form 3 April 2003; accepted 7 May 2003

Abstract

Adsorption of water soluble lead on polymetallic sea nodule has been studied in detail. Complete decontamination of lead is possible by appropriate sea nodule dosing. Adsorption is also dependent on pH and best adsorption is achieved at pH 6. Beyond pH 6, the desorption of lead from sea nodule surface is practically zero. Residual metal concentrations in the filtrate after adsorption is negligible. Both Freundlich and Langmuir isotherms may reasonably explain adsorption of lead on sea nodule. Chemically bound moisture plays a very crucial role in lead adsorption. Lead adsorptive capability of sea nodule is practically destroyed when calcined at a temperature of 900°C. Lead loading capacity of sea nodule has been estimated at 440 mg of lead per gram of sea nodule. The performance of sea nodule as a lead adsorbent has been successfully tested over six simulated lead contaminated water systems. Lead loading capacity of sea nodule compares favorably with other adsorbents like activated carbon, ion exchange resin, anionic clay, granulated blast furnace slag and natural and treated zeolites.
© 2003 Elsevier Ltd. All rights reserved.

Keywords: Adsorption; Lead; Sea nodule; Chemically bound moisture; pH_{ZPC}

1. Introduction

Lead is a recognized environmental pollutant that acts as a cumulative poison. Inorganic Pb^{2+} is an enzyme inhibitor, which also affects the nervous system. The major environmental sources of metallic lead and its salts and oxides are paints and pigments, battery industries, lead smelters, etc. Once mobile in the environment in ionic form, like many other toxic elements it finds its way into the human body through drinking water, food and air. Limit values of lead in drinking water and surface water intended for drinking, as set by EU, USEPA and WHO, are 10, 50 and 10 μg/l, respectively [1]. However, more recently an EPA document prescribes a zero lead value in national primary drinking water standard [2]. In India, limit value of lead in drinking water is 0.01 mg/l [3].

Removal of lead from contaminated water bodies has been attempted by several researchers employing a wide variety of techniques. Majority of these are adsorption on various surfaces like activated carbon [4–6], peat [7], goethite mineral [8], hydrated iron and aluminium oxide [9], granular iron oxide [10], synthetic anionic clay [11], biopolymers [12], industrial wastes like red mud [13], granulated blast furnace slag [14], naturally occurring and treated zeolites [15] and coral sand [16]. Other lead removal techniques include hydrocerrusite precipitation [17], precipitation with sodium di-(*n*-octyl) phosphinate [18], precipitation with recycled alum sludge [19], ion exchange [20], electrokinetic decontamination [21] and use of microorganism [22].

Polymetallic sea nodule is an exotic naturally occurring mineral found in the large stretches of Pacific, Atlantic and Indian Ocean. This mineral has been viewed by many as the future reserve for Cu, Co and Ni.

*Corresponding author. Tel.: +91-657-271-709-14; fax: +91-657-270-527.

E-mail address: santanu@nmlindia.org, drsantanub@yahoo.com (S. Bhattacharjee).

0043-1354/03/$ - see front matter © 2003 Elsevier Ltd. All rights reserved.
doi:10.1016/S0043-1354(03)00315-4

Our laboratory studies revealed that sea nodule is a good adsorbent for a number of cations and anions. A systematic study has been reported in the present communication in which removal of lead from contaminated water bodies has been looked into using polymetallic sea nodule as adsorbent. The objective of the present study was to generate basic data on the adsorptive capability of sea nodule with reference to lead in aqueous medium.

2. Experimental

2.1. Adsorbent

Sea nodule used in the present study was collected from the Non-Ferrous Processing Division of National Metallurgical Laboratory, Jamshedpur. The material was powdered and washed with de-ionised water to remove foreign materials, dusts and fines.

2.2. Instrumental

JEOL JSM 840 A Scanning Electron Microscope with CAVEX 8000 EDS was used for identifying the material matrix. Trace elemental analyses such as Fe, Mn, Cu, Co and Ni were carried out with GBC, *Avanta* atomic absorption spectrometer (AAS). Silica, manganese and iron were analysed by conventional wet chemical methods [23–25]. Lead was analysed by GBC *Avanta* atomic absorption spectrometer; detection limit of Pb in flame AAS is 10 ppb [26]. X-ray diffractograms were taken in a Siemens D-500 X-ray Diffractometer.

2.3. Reagents

The reagents used were all of analytical grade. Stock lead solution (1000 mg/l) for adsorption study was always prepared fresh from AR grade lead nitrate [$Pb(NO_3)_2$]. 18 MΩ ASTM Grade 1 water was used for making the solutions. AAS was calibrated with lead standards prepared from Johnson Mathey specpure lead.

2.4. Batch adsorption experiments

All adsorption experiments were carried out in batches. A 100 ml of synthetic Pb solution of predetermined concentration was taken in a 250 ml stoppered conical flask. A quantity of adsorbent with a particular particle size was added to this solution and shaken in a mechanical shaker for a definite period of time. Adsorption parameters, namely, adsorbent dose, particle size, shaking time, etc., were optimized by the method of continuous variation. For optimization, adsorbent dose was varied between 0 and 1 g, particle size between 75 and 250 μm and shaking time between 0 and 300 min. After shaking, the solution was allowed to settle for 1 h, filtered and analysed for lead. The difference in the lead content before and after adsorption represented the amount of Pb adsorbed by sea nodule.

2.5. Optimization of adsorption parameters

Adsorption dose, particle size and shaking time were optimized for maximum adsorption by the method of continuous variation following batch adsorption experiments mentioned above. Optimum adsorbent dose and particle size were found to be 0.2 g and 75 μm, respectively, for 100 ml of 206 ppm lead solution. For all practical purpose equilibrium was reached within 30 min. In all subsequent experiments, unless otherwise stated, shaking time was set at 30 min.

2.6. Experiments for studying adsorption kinetics

For adsorption kinetics a different set of experiments was carried out in which 100 ml of 226.8 ppm Pb solution was adsorbed on 0.05 g of sea nodule with a particle size of 75 μm over a time period of 0–300 min following the procedure outlined in Section 2.4.

3. Results and discussion

3.1. Characterization of sea nodule

Fig. 1 shows the EDX microanalysis of sea nodule. It is evident from Fig. 1 that the major constituents of sea nodule are Mn, Fe and Si with traces of Ni, Ca, K and Mg. The SEM data are further augmented with complete quantitative chemical analyses of constituent metals, which are given in Table 1 as oxides.

To ascertain the mineral phases present in the sea nodule matrix, it was subjected to XRD analysis. The diffractogram has been shown in Fig. 2. It may be seen that there are only two discernible peaks which correspond to silica ($d = 3.34$) and a shifted β-MnO_2 ($d = 3.18$) phase. In addition to these two, one may also observe three broad bands around d-spacings of 4.85, 2.45 and 1.42, which could not be identified with any particular phase but in all likelihood were due to some hydrated oxides of Fe and Mn as will be seen being vindicated in the later part of our discussion. It is, however, apparent from the diffractogram that the compounds of Fe and Mn present in sea nodule were primarily non-crystalline in nature.

Sea nodule is extremely hygroscopic in nature. The loss on ignition (LOI) in sea nodule was found to be 20.3% of which 12.2% was free moisture. Chemically bound moisture in sea nodule plays a significant role in

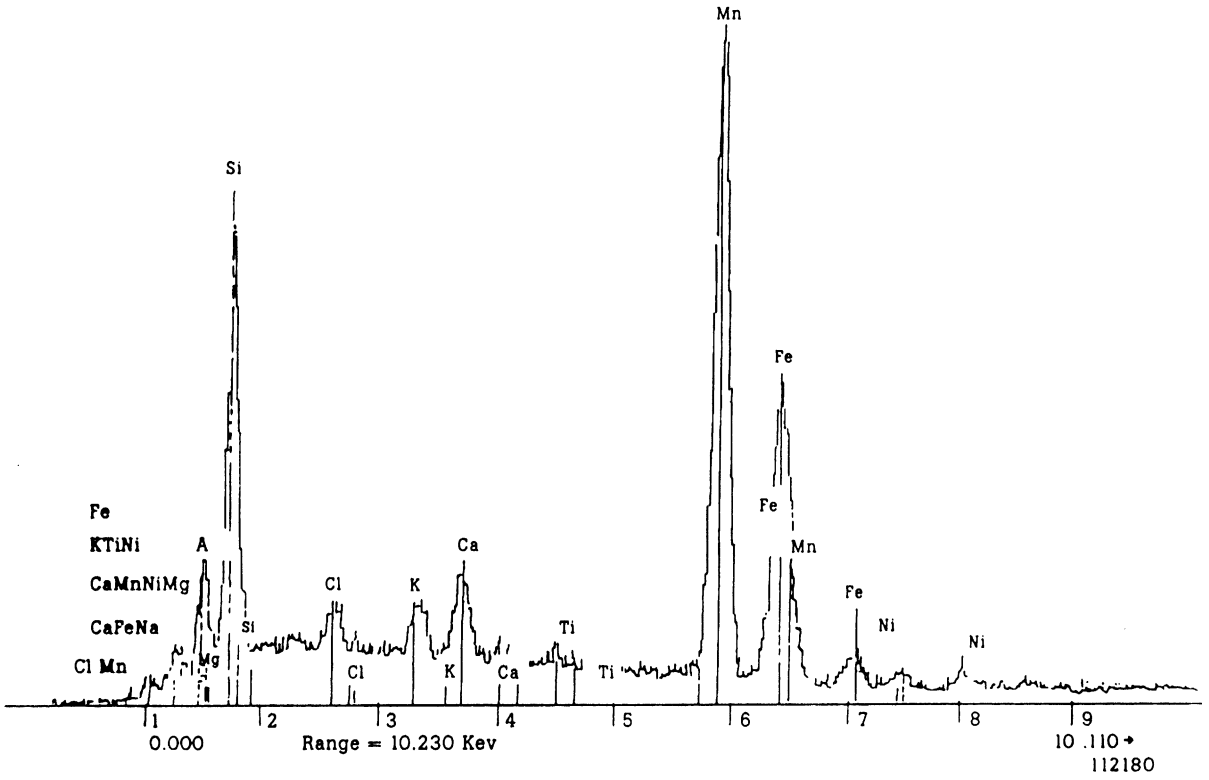

Fig. 1. SEM microanalysis of sea nodule.

Table 1
Quantitative chemical analyses of sea nodule

Element as oxide	Composition (%)
Fe_2O_3	21.2
MnO_2	31.8
SiO_2	14.2
Al_2O_3	1.9
Na_2O	3.4
CuO	0.3
NiO	0.4
MgO	3.7
CaO	2.5
CoO	0.06
LOI	20.3
Free moisture	12.2

lead adsorption and will be discussed at length in the later part of our discussion.

3.2. Adsorption isotherms

Fig. 3 shows the adsorption profiles of five different concentration of Pb in the range of 18–206 ppm with varying weights of sea nodule. Other adsorption parameters have also been shown in Fig. 3. It may be seen that Pb could be removed almost completely ($\cong$99%) from all the solutions with an orderly dose of sea nodule depending upon initial Pb concentration. Higher Pb concentration demanded higher dosing of sea nodule. Adsorption isotherms for this set of data were thus developed only within the adsorbent range which effected complete Pb removal.

Both Freundlich and Langmuir isotherms are normally considered for explaining the adsorption of metal ions on naturally occurring minerals. Freundlich and Langmuir isotherm forms, as used in the present work, are given below:

Freundlich isotherm

$$X/m = kC_e^{1/n}, \tag{1}$$

where, X is the amount of adsorbate adsorbed, m the amount of adsorbent, C_e the equilibrium concentration of the adsorbate in the solution and k the constant.

Langmuir isotherm

$$Q_e = (bV_mC_e)/(1 + bC_e), \tag{2}$$

where $Q_e = X/m$ and C_e, X and m have the same meaning as described in Freundlich isotherm, b is the constant that represents adsorption bond energy, and V_m the constant that represents maximum adsorption density corresponding to a monolayer covering the surface of the adsorbent.

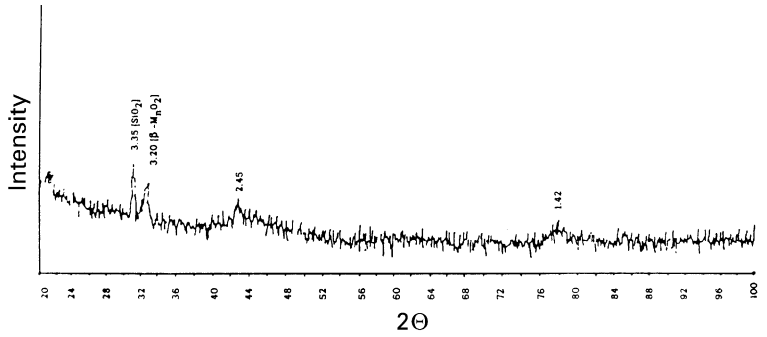

Fig. 2. X-ray diffractogram of sea nodule.

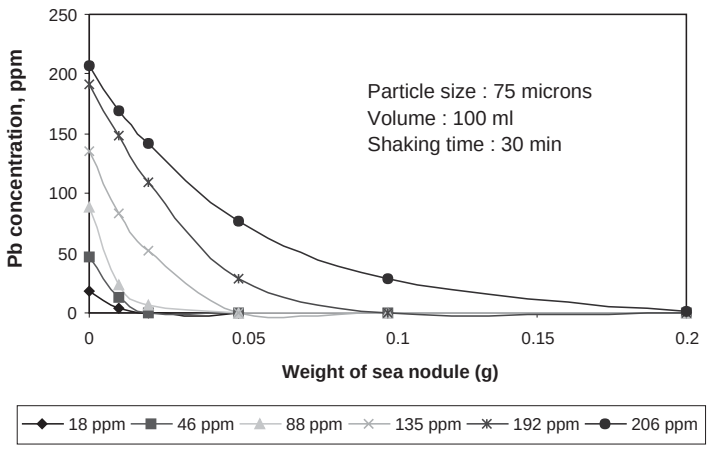

Fig. 3. Pb adsorption profile of sea nodule.

Table 2
Freundlich and Langmuir isotherm constants at different lead concentration

Initial Pb conc., C_0 (ppm)	Freundlich			Langmuir		
	k	n	r^2	V_m (mg g^{-1})	b (ml mg^{-1})	r^{2a}
206	133.9	5.4	0.8714	323.8	0.7	0.8629
192	249.6	9.8	0.9803	390	14.8	0.825
135	279.0	8.1	0.9861	467.3	2.5	0.9109
88	228.1	3.0	0.9420	574.0	1.6	0.8654
46	262.5	14.3	0.7621	332.9	10.6	0.8026

[a] Goodness of fit between $(X/m)_{calculated}$ and (X/m).

Data presented in Fig. 3 were fit into both Freundlich and Langmuir forms separately using robust techniques. n, k, b and V_m values for each curve were calculated and they have been listed in Table 2 along with goodness of the fit. It is evident from Table 2 that adsorption isotherms vary with initial lead concentrations. This point has been addressed in greater detail in the later part of our discussion.

It is pertinent to mention at this stage that Freundlich isotherm is essentially an empirical relationship without a firm theoretical basis. Langmuir isotherm as applied to the adsorption of solutes on solid surface is also an extension of its original derivation. Presence of more than one mineral phase in sea nodule complicates the situation further. Also, adsorption energy in Langmuir approach is considered constant over the entire range of

adsorption, which invariably is not true for soils and similar adsorbents like naturally occurring minerals [27]. In spite of these limitations, reasonable success achieved with Freundlich and Langmuir forms make them popular choice for explaining sorption experimental data.

3.3. Adsorption kinetics

The Lagergren first-order rate equation [28], as applied by Ho and Mckay [7], was used to explain the adsorption kinetics of lead on sea nodule. The Lagergren form may be written as

$$\log(q_\infty - q_t) = \log(q_\infty) - (k/2.303)t, \quad (3)$$

where q_∞ is the amount of adsorbate adsorbed per unit weight of the adsorbent at equilibrium ($t = \infty$), q_t the amount of adsorbate per unit weight of adsorbent at time t.

Experiments carried out to study adsorption kinetics have been discussed in Section 2.6. Both q_∞ and q_t have been expressed as mg/g and q_t value at 300 min has been considered as q_∞. Plot of log $(q_\infty - q_t)$ with time t has been shown in Fig. 4. Also shown in Fig. 4 are the rate equation and goodness of the fit (r^2). Excellent linear fit in Fig. 4 clearly indicates that the adsorption of lead on sea nodule follows a first order kinetics. In Eq. (3), the intercept should be equal to $\log(q_\infty)$. However, from Fig. 4, one may find the intercept to be 2.14 as opposed to the experimental value of 2.3. This, however, is not uncommon in real situations as also observed by Ho and Mckay [7] who improved the Lagergren fit with a pseudo-first-order rate equation. The approach of Ho and McKay comprises two steps. In the first step, an optimum equilibrium sorption capacity q_∞ is obtained by some trial and error method and in the second, new correlations are drawn by replacing t in Eq. (3) with $(t + t_0)$ where t_0 is an adjustable parameter and replacing q_∞ with the optimum q_∞. The approach of Ho and Mckay as applied to the present work and improvement obtained thereupon are shown below.

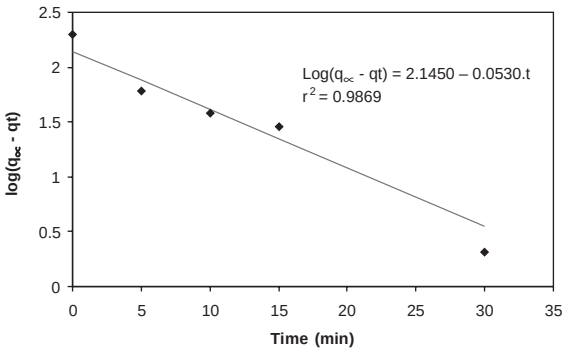

Fig. 4. Lagergren plot for first order kinetics.

Considering $q_\infty = 200.9$ at $t = 300$ min, one gets the following correlation equation (Fig. 3):

$$\log(q_\infty - q_t) = 2.1450 - 0.0530t \quad (r^2 = 0.9869,\ q_\infty^{\text{extrapolated}} = 139.6) \quad (4)$$

$q_\infty^{\text{extrapolated}}$ in Eq. (4) is much less than the $q_\infty = 200.9$. q_∞ was further manipulated by a trial and error method which resulted into a slightly better correlation equation with an optimum $q_\infty = 200.8$. The correlation equation thus obtained has been shown below.

$$\log(q_\infty - q_t) = 2.2137 - 0.0594t \quad (r^2 = 0.9927,\ q_\infty^{\text{extrapolated}} = 163.6) \quad (5)$$

Comparison of Eqs. (4) and (5) clearly indicates that the choice of q_{300} as q_∞ in the present case was a fairly reasonable one. This also shows that Eq. (5), which is an improvement over Eq. (4), fails to match $q_\infty^{\text{extrapolated}}$ with q_∞. Fresh correlations were drawn by replacing t with $(t + t_0)$ in Eq. (5) and a q_∞ of 200.8, where t_0 was an adjustable parameter. Best correlation was obtained with a t_0 value of 1.5 for which the correlation equation was

$$\log(q_\infty - q_t) = 2.3027 - 0.0594t \quad (r^2 = 0.9927,\ q_\infty^{\text{extrapolated}} = 200.77) \quad (6)$$

This may be noted that though there was no improvement in the r^2 value in Eq. (6) over Eq. (5), $q_\infty^{\text{extrapolated}}$ improved significantly and was almost at par with q_∞.

3.4. Loading study

Loading capacity of an adsorbent at a particular level of adsorption may be defined as the maximum amount of adsorbate per unit weight of the adsorbent for defined adsorption parameters. Loading of sea nodule with lead (X/m) was calculated for various Pb concentrations at different adsorbent dose for the data presented in Fig. 3 and these have been listed in Table 3 with corresponding level of Pb removal. It was interesting to note that at 90% Pb removal (interpolated) lead loading (X/m) was a function of initial lead concentration, which has also been demonstrated in Fig. 5. This, however, was expected as it was observed in Section 3.2 that adsorption isotherms were different for different initial concentrations. Maximum Pb loading was observed with 88 ppm Pb solution at which Pb loading capacity of sea nodule was estimated at 440 mg/g. It was further gratifying to note in Table 2 that V_m, one of the Langmuir isotherm constants, which is also an estimate of the sorption capacity of the adsorbent passes through a maximum at around 88 ppm lead solution.

Table 3
Lead loading at various lead concentrations and varying sea nodule dose

Sea nodule (g)	Initial Pb conc., C_0 (ppm)											
	18		46		88		135		192		206	
	% Ads.	X/m	% Ads.	X/m	% Ads.	X/m	% Ads.	X/m	% Ads.	X/m	% Ads.	X/m
0.01	79.35	147.38	77.7	332.8	74.21	659.1	38.15	514.6	22.48	431.72	18.02	371.9
0.02	>99.5	92.86	>99.5	230.9	92.35	410.1	61.55	415.1	42.80	410.95	31.48	324.8
0.05	>99.5	36.93	>99.5	92.57	>99.5	177.2	>99.5	268.6	84.74	325.5	62.77	259.1
0.1	>99.5	18.43	>99.5	46.65	>99.5	88.69	>99.5	134.8	>99.5	191.97	86.43	178.4
0.2	>99.5	9.18	>99.5	23.11	>99.5	44.26	>99.5	67.43	>99.5	95.7	>99.5	102.8
0.3	>99.5	6.10	>99.5	15.43	>99.5	29.48	>99.5	44.87	>99.5	64.01	>99.5	68.5
0.4	>99.5	4.57	>99.5	11.57	>99.5	22.11	>99.5	33.59	>99.5	47.71	>99.5	51.54
0.5	>99.5	3.67	>99.5	9.26	>99.5	17.69	>99.5	26.89	>99.5	38.25	>99.5	41.17

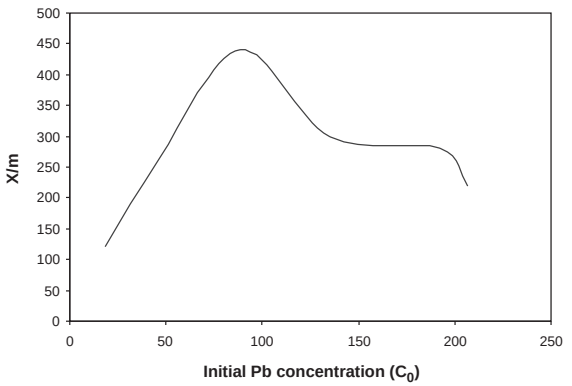

Fig. 5. Variation of lead loading with initial lead concentration.

3.5. Residual metal concentrations

Since sea nodule is a composite matrix of primarily Fe, Mn, Cu, Co and Ni, the residual concentrations of these elements in the filtrate after adsorption is of paramount importance. The filtrates obtained during loading study for different Pb concentrations with varying sea nodule doses were also analysed for Mn, Fe, Cu, Co and Ni in addition to Pb. The results for 18, 46 and 88 ppm lead solutions have been listed in Table 4. The results for 135, 192 and 206 ppm lead have not been shown but they follow the same pattern. Also given in Table 4 is the pH of the filtrates after adsorption. It may be seen from Table 4 that except for Mn, there is no appreciable leaching of these elements from the adsorbent to the filtrate and residual concentrations of these elements in the filtrate lie well below maximum permissible levels for these elements in drinking water as per WHO guidelines. One may, however, find some amount of Mn being leached out from the adsorbent into the filtrate, which may be of some concern. Mn leaching increases with increasing Pb concentration as well as sea nodule dosing. Nevertheless, as may be seen from Table 4 that up to 0.1 g of sea nodule in all the contaminated solutions residual Mn concentration was less than 0.5 ppm, maximum permissible value of Mn in drinking water by WHO standard. It was further interesting to note in Table 4 that there was a distinct rise in the solution pH on increasing sea nodule dose. It was indicative of the fact that Pb adsorption in seanodule was associated with release of some OH^- ions. It is also worthwhile to mention at this point that sea nodule was found to adsorb some amount of NO_3^- ions. Role of anions on the overall lead adsorption process on sea nodule is being investigated in further detail by the present group of investigators.

3.6. Adsorption and desorption at different pH

Adsorption and desorption of lead on sea nodule were studied in the pH range of 2–8. For adsorption, procedure outlined in the experimental section was followed with 0.05 g of adsorbent and 100 ml of 80 ppm aqueous lead solution at a desired pH. pH was adjusted with dilute HNO_3 and dilute NaOH. For desorption, initial adsorption was carried out with 0.05 g of the adsorbent and 100 ml of 80 ppm aqueous lead solution at the pH of the solution. Thereafter, the pH of the solution was adjusted to the desired pH by controlled addition of dilute HNO_3 or dilute NaOH. The entire solution was shaken further for half an hour in a mechanical wrist shaker and allowed to settle for one more hour before it was filtered and analysed for lead.

Let C_0 be the initial Pb concentration of the solution in ppm (mg/l), C_e be the equilibrium Pb concentration in ppm at a particular pH, C'_e be the equilibrium Pb concentration of the solution at a particular pH after desorption.

Table 4
Residual metal concentrations in the filtrate after lead adsorption

Initial Pb conc., C_0 (ppm)	Sea nodule dose (g)	pH after adsorption	Mn (ppm)	Zn (ppm)	Cu (ppm)	Co (ppm)	Ni (ppm)	Fe (ppm)
18	0	4.86	n.d.	0.01	0.01	n.d.	n.d.	n.d.
	0.01	5.05	0.01	0.01	0.01	0.01	n.d.	n.d.
	0.02	5.61	0.07	n.d.	0.01	0.01	0.01	n.d.
	0.05	6.42	0.27	n.d.	0.02	0.01	n.d.	0.06
	0.1	7.38	0.30	n.d.	0.02	0.01	0.01	0.11
	0.2	8.32	0.55	n.d.	0.04	0.01	0.02	0.28
	0.3	8.57	0.77	0.01	0.06	0.01	0.05	0.43
	0.4	8.71	1.11	0.01	0.07	0.02	0.07	0.54
	0.5	8.72	1.23	0.01	0.07	0.02	0.07	0.55
46	0	4.8	n.d.	0.01	n.d.	n.d.	n.d.	n.d.
	0.01	4.94	0.07	n.d.	n.d.	0.01	n.d.	n.d.
	0.02	5.18	0.14	n.d.	n.d.	0.01	n.d.	0.02
	0.05	5.86	0.26	n.d.	0.01	n.d.	n.d.	0.02
	0.1	6.52	0.37	n.d.	0.04	n.d.	0.05	0.26
	0.2	7.54	0.71	n.d.	0.06	n.d.	0.03	0.06
	0.3	8.08	1.12	0.01	0.07	n.d.	0.07	0.27
	0.4	8.32	1.57	0.01	0.07	n.d.	0.07	0.17
	0.5	8.42	1.78	0.02	0.08	n.d.	0.08	0.14
88	0	4.72	n.d.	0.01	n.d.	n.d.	n.d.	n.d.
	0.01	4.74	0.12	n.d.	n.d.	n.d.	n.d.	n.d.
	0.02	4.77	0.17	n.d.	0.01	n.d.	n.d.	n.d.
	0.05	5.32	0.31	n.d.	0.01	0.01	0.3	n.d.
	0.1	5.89	0.40	n.d.	0.02	0.01	0.03	0.02
	0.2	6.76	0.86	0.04	0.03	0.02	0.04	0.24
	0.3	7.48	1.37	0.05	0.06	0.02	0.05	0.34
	0.4	7.93	1.89	0.05	0.08	0.02	0.09	0.53
	0.5	8.13	1.98	0.05	0.10	0.02	0.09	0.60

n.d. = Not detectable (below detection limit); detection limit for Pb = 10 ppb; Ca, Cu, Mn = 1 ppb; Zn = 0.8 ppb; Fe = 3 ppb [26].

Then

$$(C_0 - C_e)/10 = \text{Amount of Pb adsorbed in mg (for 100 ml)}, \quad (7)$$

$$(C'_e - C_e)/10 = \text{Amount of Pb desorbed in mg (for 100 ml)}. \quad (8)$$

Fig. 6 shows the adsorption–desorption curves of sea nodule with lead in the pH range of 2–8. Lead adsorption increases on increasing the solution pH and reaches a maximum at pH 6. Similarly desorption decreases on increasing pH and beyond pH 6 lead is practically not released from the adsorbent. This clearly indicates that at or beyond pH 6, sea nodule may be used as a potential adsorbent of lead in contaminated water bodies. It is also apparent from Fig. 6 that the Pb-sea nodule sludge generated may be safely disposed in an environment where pH is greater than 6.

It is important to note at this point that the solubility product of $Pb(OH)_2$ is 2×10^{-16}. It may be calculated

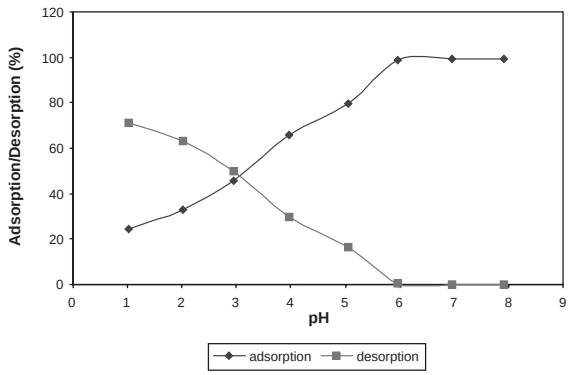

Fig. 6. Adsorption and desorption of lead by sea nodule at varying pH.

and has been checked experimentally that at pH 6, entire lead should remain in the solution as Pb^{2+} throughout the concentration range (0–210 ppm) at which present study was carried out. At still higher pH however, part

of the lead may precipitate out as $Pb(OH)_2$ which also depends upon lead concentration. Since maximum adsorption was achieved at a pH of 6, It may be safely stated that lead removal at or below pH 6 was by the process of adsorption and not precipitation.

It was even more interesting to note that $Pb(OH)_2$ at a still higher pH goes into the solution as plumbite anion, PbO_2^{2-}. It was most gratifying to note that sea nodule was also a good adsorbent for PbO^{2-}. The ramifications for this observation are enormous and calls for a complete investigations which has already been taken up by the present group of investigators. The role of OH^- and other anions on the lead adsorption is being investigated giving due consideration to material balance as well as electro-neutrality in the solution.

Residual elements like Fe, Co, Cu, Ni and Mn were also analysed in the filtrate obtained from adsorption and desorption experiments. It was noted with satisfaction that concentrations of these elements in the filtrate beyond pH 6 were well below the maximum permissible levels of these elements in drinking water as per WHO guidelines.

3.7. Adsorbent regeneration/sludge disposal

In a wastewater treatment that uses adsorption, regeneration of the adsorbent and/or disposal of the sludge is crucially important. Attempts were made to regenerate the spent sea nodule by stripping of the lead from sea nodule surface using different concentrations of acetic acid and potassium iodide. Potassium iodide failed and only partial success was achieved with acetic acid which also was much short of desired level.

It has already been mentioned that removal of Pb^{2+} from solution using sea nodule as adsorbent follows two pathways. At lower pH it is adsorption of Pb^{2+} ions over solid surface and at higher pH, it is partially adsorption and partially precipitation as $Pb(OH)_2$. The fine particles of $Pb(OH)_2$ have a tendency to settle over the solid sea nodule surface. Thus the pH at which the sludge is generated is also important for a probable regeneration scheme. Instant solubility of $Pb(OH)_2$ in acetic acid may be attributed to the partial success obtained with acetic acid in regenerating sea nodule sludge. Acetic acid, however, failed to drive out the Pb^{2+} ions adsorbed over sea nodule surface.

3.8. Chemically bound moisture in sea nodule

Any moisture trapped in a matrix beyond 105°C is normally termed as chemically bound moisture. This may be due to water of crystallization, hydration of oxides or chemically bound hydroxyl groups. Chemically bound moisture figures in the conventional determination of LOI at 900°C, but may also include other volatiles.

It was mentioned earlier (Section 3.1) that the chemically bound moisture might play an important role in Pb adsorption, which was looked into systematically in greater detail. Sea nodule samples were calcined at varying temperatures of 100°C, 200°C, 300°C, 500°C, 700°C and 900°C. The calcined products and the untreated sea nodule were subjected to X-ray analysis and their diffractograms have been shown in Fig. 7 which makes some very interesting revelations. The diffractogram of untreated sea nodule has been discussed earlier in detail while discussing Fig. 2 but also retained here for the sake of quick comparison. This pattern broadly remains unchanged with calcined products upto 500°C not withstanding some distinct and progressive changes along the entire spectrum. The wide band observed around $d = 4.85$ gets resolved into a number of small but distinct peaks with increasing calcination temperature. Maximum number of such peaks could be observed at 200°C which smoothened on increasing the temperature and eventually settled at two distinct peaks at $d = 4.25$ and 4.85 at 500°C corresponding to SiO_2 and Mn_3O_4 phases, respectively. Intermediate peaks at $d = 4.97$ for 200°C and 300°C products correspond to some non-stoichiometric intermediate phase Mn_xO_y, which gets converted to Mn_3O_4 on increasing the calcination temperature. At 500°C one may also observe the beginning of several other peaks, which transpires into very well-defined peaks of Mn_3O_4 and β-Fe_2O_3 at 700°C and 900°C. It was most interesting to observe that in the entire range of calcined products a consistent peak at around $d = 3.15-3.22$ could be observed which was almost independent of calcination temperature. This peak was identified with β-MnO_2, which was also supported by the identification of auxiliary peaks of β-MnO_2. It was also interesting to note that the most predominant peak of silica in untreated sea nodule was completely suppressed at 900°C as its relative intensity considerably decreased due to the formation of several new and intense peaks.

Effect of calcination on lead adsorptive capability of sea nodule was also studied in detail. Calcined products of each of 0.1 g was separately used for Pb adsorption in 100 ml of 242.4 ppm lead solution keeping other adsorption parameters constant in each. Lead removals for each calcined product have been shown in Table 5. Also shown in Table 5 are the chemically bound moistures in each of the calcined products and residual Mn, Ni, Co and Cu contents in the filtrate after adsorption. It may be seen that lead adsorptive capability of sea nodule increases slightly at 100°C after which it sharply declines on increasing the calcination temperature resulting into removal of chemically bound moisture. The increase in lead adsorptivity at 100°C may be attributed to the removal of free moisture which amounts to 12.2%. At 900°C where chemically bound moisture was practically non-existing, calcined sea nodule had almost ceased to adsorb lead.

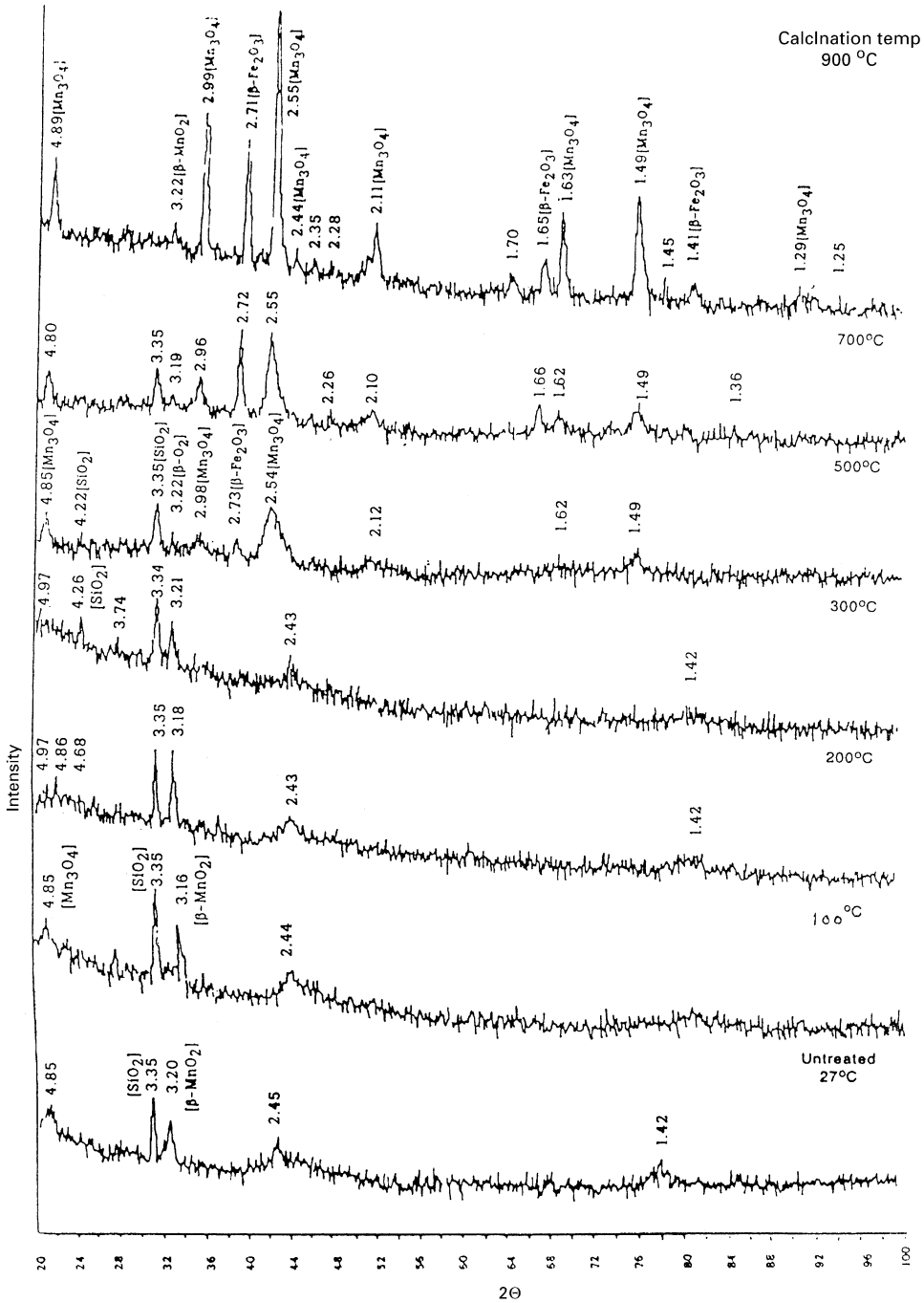

Fig. 7. X-ray diffractograms of various calcined products of sea nodule.

Steady decline in the lead adsorptive capacity of sea nodule with decreased chemically bound moisture further highlights the role played by hydroxy groups in sea nodule towards adsorbing lead.

A strong linear correlation could be derived between Pb adsorption and chemically bound moisture in the range of 100–900°C:

$$\beta = 5.5384\alpha + 3.7198 \quad (9)$$

($r^2 = 0.9900$; $n = 6$), where β is the lead removed expressed as percentage, α is the chemically bound moisture expressed as percentage.

Table 5
Effect of calcination temperature on lead adsorption by sea nodule

Adsorbent weight: 0.1 g; Pb concentration: 242.2 ppm; volume 100 ml.

Calcination temperature (°C)	Chemically bound moisture (%)	Pb removal (%)	Fe (ppm)	Mn (ppm)	Ni (ppm)	Co (ppm)	Cu (ppm)
27	20.3	45.7	n.d.	0.26	0.05	0.02	0.28
100	8.1	47.8	n.d.	0.28	0.01	0.01	0.27
200	5.6	34.3	n.d.	0.07	n.d.	0.02	0.09
300	4.3	30.9	n.d.	0.09	n.d.	0.01	0.07
500	2.4	15.9	n.d.	n.d.	n.d.	n.d.	n.d.
700	0.97	7.6	n.d.	n.d.	n.d.	n.d.	n.d.
900	0	4.5	n.d.	n.d.	n.d.	n.d.	n.d.

n.d. = Not detectable (below detection limit).

Chemically bound moisture could also be correlated with the calcination temperature by the following non-linear correlation:

$$\alpha = 10^{-5}\gamma^2 - 0.0203\gamma + 9.6644 \quad (10)$$

($r^2 = 0.9911$; $n = 6$), where γ is the calcination temperature in °C

It is also possible to correlate lead removal (β) with calcination temperature (γ) linearly although the fit is inferior to the one observed in Eq. (9). A parabolic non-linear fit of lead removal (β) with calcination temperature (γ) is, however, at par with Eq. (9).

The impressive correlation Eq. (9) clearly highlights the underlying fundamental relationship between lead removal and chemically bound moisture. It was gratifying to note that residual concentrations of Mn, Ni, Co and Cu in the filtrate after Pb adsorption with calcined products were small in general and decreased even further with increasing calcination temperature. This was due to the formation of insoluble metal oxides which was also supported by their respective diffractograms.

3.9. pH_{zpc} of sea nodule

pH_{zpc} (pH at zero point charge) is an indicator of the net surface charge of the adsorbent and its preference for ionic species. pH_{zpc} of the seanodule used in the present work was determined as 7.4 by the method of Huang and Ostavic [29]. It has already been established that sea nodule contains a significant amount of chemically bound moisture. It has also been ascertained that the compounds of Fe and Mn in sea nodule are non-crystalline at room temperature and in all likelihood exist as their oxy hydroxides. Goethite, oxy hydroxide of iron with the chemical formula α-FeO(OH) has a pH_{zpc} of 8.6 and is known to be a good adsorbent of anion like arsenite and arsenate [30]. Silica, another mineral phase of sea nodule has a pH_{zpc} of 2.3 while oxy hydroxide of Mn, MnOOH also has a pH_{zpc} of 2.3 [31]. It follows from the above discussion that sea nodule surface has both positive and negative sites and the observed pH_{zpc} of 7.4 is a net combination of all such sites. A direct and convincing evidence in favour of this argument was observed when sea nodule was found to adsorb anions like arsenite and arsenate exceedingly well, the results of which will be communicated at a later date.

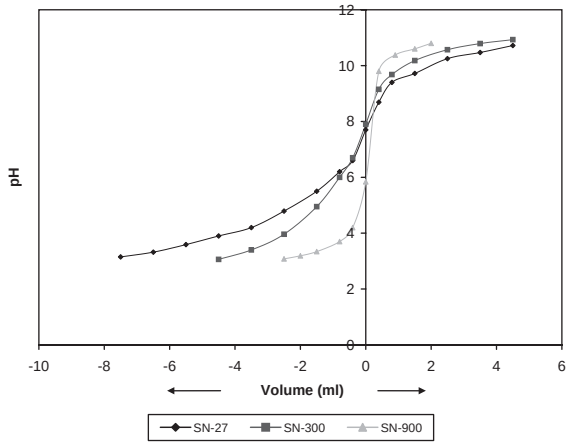

Fig. 8. pH_{zpc} curves of various calcined products of sea nodule.

pH_{zpc} of different calcined products were determined and it was observed that pH_{zpc} increased on increasing the calcination temperature. For example, pH_{zpc} of sea nodule calcined at 900°C was 8.0 which was a clear evidence of the destruction of negative sites at the surface of sea nodule with increasing temperature which eventually manifested itself in the reduced lead adsorption capability as shown in Table 5.

pH_{zpc} curves of sea nodule as received at 27°C (SN-27) and calcined at 300°C (SN-300) and 900°C (SN-900) have been shown in Fig. 8 following the method of Huang and Ostavic [29]. It may be seen that the pH curves become sharper with increasing calcination temperature. This reflects the depleted buffering action of adsorbent surface with increasing temperature which is normally associated with the charged sites at the surface.

3.10. Lead adsorption mechanism

Probable lead adsorption mechanism over sea nodule surface may not be very straight forward as sea nodule matrix contains a number of mineral phases as has been discussed in Sections 3.8 and 3.9.These mineral phases have different types of surface charge and can adsorb different types of ions. -FeOOH, a principal mineral phase of sea nodule with a pH_{zpc} of 8.6 has positive charge on the surface that can attach anions like arsenite and arsenate. This also implies that with regard to arsenate and arsenite anions, -FeOOH should work better at a pH below 8.6 and its efficiency should go down at pH above 8.6 where OH^- ions neutralise the surface positive charge and render it less effective for anions. This indeed was observed with regard to arsenate adsorption on ferrihydrites [32]. Similarly, MnOOH, another mineral phase of sea nodule having a pH_{zpc} of 2.3, has negative charges in its surface and normally should attach cations. However, the surface of MnOOH may be modified by exposing it to cationic environment so that it can also adsorb anions [30,31]. Any lead adsorption mechanism on sea nodule must take into account these factors.

A probable lead adsorption mechanism over sea nodule must also accommodate following experimental observations. A scrutiny of Table 4 reveals that on increasing sea nodule dose, solution pH slowly increases. It may also be observed that for the same sea nodule dose, residual Mn concentration keeps on building up on increasing the initial lead concentration. Lead adsorption capability of sea nodule is directly related to the hydroxy groups present in the sea nodule. Sea nodule was also found to adsorb some amount of nitrate anion during the process of adsorbing Pb^{2+}. Plumbite anion, PbO_2^{2-} was found to have been readily adsorbed over the sea nodule surface at a pH of 11.

In all likelihood Pb^{2+} gets adsorbed on the MnOOH surface resulting into the release of Mn^{2+} ions, which keeps on building up as initial lead concentration increases. Since all the experiments, barring adsorption/desorption study, were carried out at pH < 7, surface of FeOOH might got modified with H^+ ions present in the solution by way of coupling with the surface OH groups, resulting into net increase in solution pH. Adsorption of NO_3^- ions over FeOOH surface might also contribute to pH increase by way of OH^- release. Present mechanism of lead adsorption over sea nodule is somewhat qualitative in nature as an exhaustive mechanism must take into consideration the complete material balance and electro-neutrality of the solution.

3.11. Performance of sea nodule as lead adsorbent

Performance of an adsorbent with respect to an adsorbate may be judged by its loading capacity, which has been defined earlier in Section 3.4. Lead loading capacity of sea nodule as such compares favorably with lead adsorbents like layered double hydroxide [11], natural zeolite, 91.17 mg/g [15], granulated blast furnace slag, 20–25 mg/g [14], etc. A true comparison between different adsorbents, however, requires treatment of the same input water with different adsorbents under identical sets of adsorption parameters in addition to other factors like price of the adsorbent, experimental set up, ease of filtration, etc.

Table 6
Performance of sea nodule as a lead adsorbent over simulated water matrix

Water sample	Adsorption	Pb (ppm)	Fe (ppm)	Ca (ppm)	Mg (ppm)	Mn (ppm)	Zn (ppm)
A	Before	n.d.	0.65	18.51	20.1	0.7	1.74
	After	n.d.	n.d.	14.79	17.52	0.05	0.12
B	Before	2.9	0.58	18.1	20.2	0.69	1.78
	After	n.d.	n.d.	14.25	17.75	0.05	1.16
C	Before	7.1	0.51	19.0	20.44	0.67	1.78
	After	n.d.	n.d.	15.0	18.05	0.08	0.21
D	Before	13.9	0.76	18.73	20.41	0.67	1.78
	After	n.d.	n.d.	14.97	18.18	0.11	0.30
E	Before	18.3	0.93	19.63	20.37	0.67	1.78
	After	n.d.	n.d.	16.83	19.0	0.34	0.67
F	Before	26.3	0.96	19.0	20.2	0.67	1.87
	After	n.d.	n.d.	16.5	20.16	0.41	0.94

n.d. = Not detectable (below detection limit).

The performance of sea nodule as a lead adsorbent was adjudged over a number of simulated water samples prepared by mixing different quantities of Fe, Ca, Mg, Mn and Zn in addition to lead. Each of these mixtures of 50 ml was treated with 0.05 g of the adsorbent for a period of 30 min in a manner used for other batch adsorption experiments described earlier in Section 2.4. Metal contents were analysed before and after adsorption the result of which has been given in Table 6. It may be seen that in each of these mixtures lead could be removed completely (below detection limit 0.01 mg/l). It was most interesting to observe that sea nodule was also a good adsorbent for Fe, Zn and Mn and a mild water softener. Removals of Zn and specially Mn were inversely correlated with the lead concentration in water. However, Fe removal was independent of Pb concentration.

3.12. Scope of real life application

This study looks into the basic lead adsorptive capability of sea nodule and the chemical species responsible for it. It is possible to synthesize them in the laboratory and develop an even more potent lead adsorbent. Scarce availability of sea nodule may be a deterrent in using the material directly as an adsorbent. Nevertheless, very high lead loading capacity of sea nodule makes the synthetic route to be of high relevance. Laboratory synthesis of lead active components in sea nodule is already in progress at National Metallurgical Laboratory, Jamshedpur, India.

4. Conclusion

A batch adsorption study has been reported on the adsorption of water soluble lead on polymetallic sea nodule. Sea nodule is a hygrosopic complex mixture of oxy hydroxides of Fe and Mn. It is possible to remove lead almost completely ($>99.5\%$) from contaminated water bodies using appropriate dose of sea nodule. Lead loading capacity of sea nodule has been estimated at 440 mg/g. Both Freundlich and Langmuir isotherm forms may be satisfactorily employed to explain lead adsorption on sea nodule, which is best at pH 6. Desorption of lead is practically zero beyond pH 6. Residual metal concentrations in the filtrate after lead adsorption, presumably leached out from the adsorbent, lie well below their respective maximum permissible levels as per WHO guidelines for drinking water. It is possible to partially regenerate sea nodule using acetic acid. Pb adsorptive capability of sea nodule may be linearly correlated with the chemically bound moisture. Sea nodule calcined at 900°C is practically stripped of its capability to adsorb lead. pH_{zpc} of calcined sea nodule increases with increasing calcination temperature. Performance of sea nodule as a lead adsorbent compares favorably with other adsorbents like activated carbon, ion exchange resin, anionic clay, natural and treated zeolite and granulated blast furnace slag. It is possible to prepare an even more potent lead adsorbent by synthesizing Pb active components in sea nodule.

Acknowledgements

The authors take this opportunity to thank Director, National Metallurgical Laboratory, Jamshedpur for his kind permission to publish this work. The authors express their gratitude to Sri K.K. Gupta, Senior Scientist, ANC Division for critically examining the manuscript. The authors also wish to thank Shri S.K. Das for EDX analysis and Shri B. Ravikumar for XRDs.

References

[1] Lead, Pollution prevention and abatement handbook. World Bank Group, Effective July, 1998, http://wbln0018.worldbank.org/essd.nsf/Global View/PPAH/$File/37_lead.pdf.
[2] Current drinking water standards, 2002, EPA. Office of water, http://www.epa.gov/safewater/mcl.html.
[3] IS (1991) Drinking water specification, (first revision) (Amendment 1) Reaffirmed 1993. IS: 10500.
[4] Akhtar S, Qadeer R. Active carbon as an adsorbent for lead ions. Adsorption Sci Technol 1997;15:815–24.
[5] Lee M-Y, Shin H-J. Removal of lead in a fixed bed column packed with activated carbon and crab shell. Sep Sci Technol 1998;33:1043–56.
[6] Mostafa MR. Adsorption of mercury, lead and cadmium ions on modified activated carbons. Adsorption Sci Technol 1997;15:551–7.
[7] Ho YS, Mckay G. The sorption of lead(II) ions on peat. Water Res 1999;33:578–84.
[8] Hayes KF, Leckie JO. Mechanism of lead ion adsorption at the goethite/water interface. In: Davis JA, Hayes KF, editors. Geochemical process at mineral surface. ACS Symposium Series, vol. 323. Washington, DC: American Chemical Society, 1986.
[9] Srivastava SK, Bhattacharjee G, Tyagi R, Pant N, Pal N. Studies of the removal of some toxic metal ions from aqueous solutions and industrial waste. Part I (removal of lead and cadmium by hydrous iron and aluminium oxide). Environ Technol Lett 1988;9:1173–85.
[10] Theis TL, Iyer R, Ellis S. Evaluating of a new granular iron oxide for removing lead from drinking water. J Am Water Works Assoc 1992;July:101–5.
[11] Seida Y, Nakano Y, Nakamura Y. Rapid removal of dilute lead from water by pyroaurite-like compound. Water Res 2001;35:2341–6.
[12] Seki H, Suzuki A. Adsorption of lead ions on composite biopolymer adsorbent. Ind Eng Chem Res 1996;35:1378–82.

[13] Gupta VK, Gupta M, Sharma S. Process development for the removal of lead and chromium from aqueous solutions using red mud—an aluminium industry waste. Water Res 2001;35:1125–34.
[14] Dimitrova SV, Mehandgiev DR. Lead removal from aqueous solutions by granulated blast-furnace slag. Water Res 1998;32:3289–92.
[15] Curkovic L, Cerjan-stefanovic S, Filipan T. Metal ion exchange by natural and modified zeolites. Water Res 1997;31:1379–82.
[16] Suzuki Y, Takeuchi Y. Uptake of a few divalent heavy-metal ion species from their aqueous solutions by coral sand heat-treated at various temperatures. J Chem Eng Jpn 1994;27:165–70.
[17] Macchi G, Marani D, Pagano M, Bagnuolo G. A bench study on lead removal from battery manufacturing wastewater by carbonate precipitation. Water Res 1996;30: 3032–6.
[18] Esalah JO, Weber ME, Vera JH. Removal of lead from aqueous solutions by precipitation with sodium di-(*n*-octyl) phosphinate. Sep Purification Technol 2000;18: 25–36.
[19] Chu W. Lead metal removal by recycled alum sludge. Water Res 1999;33:3019–25.
[20] Mier MV, Callejas RL, Gehr R, Cisneros BEJ, Alvarez PJJ. Heavy metal removal with mexican clinoptilolite: multi-component ionic exchange. Water Res 2001;35: 373–8.
[21] Chung HI, Kang BH. Lead removal from contaminate marine clay by electrokinetic soil decontamination. Eng Geol 1999;53:139–50.
[22] Leung WC, Wong M-F, Chua H, Lo W, Yu PH, Leu CK. Removal and recovery of heavy metals by bacteria isolated from activated sludge treating industrial effluents and municipal waste water. Water Sci Technol 2000;41:233–40.
[23] ASTM. Standard test method for determination of silica in manganese ores, iron ores and related materials by gravimetry (E247-96). 1996;03.05:270–71.
[24] ASTM. Standard test method for determination of iron in manganese ores by hydrogen sulfide reduction-dichromate titration (E316-95a). 1996;03.05:313–4.
[25] ASTM. Standard test method for determination of manganese (IV) in manganese ores by redox titration (E465-95a). 1996;03.06:119–21.
[26] Vandecasteele C, Block CB. Modern methods for trace element determination. Brisbane, Toronto, Singapore: Wiley, 1993. p. 134–5.
[27] Baruah TC, Patgiri DK. Physics and chemistry of soils. New Delhi: New Age International Publishers, 1996. p. 128–44.
[28] Lagergren S. About the theory of so-called adsorption of soluble substances. Kungliga Svenska Vetenskapsakademiens. Handlingar, Band 1898;24:1–39.
[29] Huang CP, Ostavic FG. Removal of cadmium(II) by activated carbon adsorption. J Environ Eng Div ASCE 1978;104:863–78.
[30] Chakravarty S, Dureja V, Bhattacharyya G, Maity S, Bhattacharjee S. Removal of arsenic from groundwater using low cost ferruginous manganese ore. Water Res 2002;36:625–32.
[31] Mok WM, Wai CM. Mobilization of arsenic in contaminated river waters. In: Nriagu JO, editor. Arsenic in the environment, Part 1. New York: Wiley; 1994. p. 99–117.
[32] Raven KP, Jain A, Loeppert RH. Arsenite and arsenate adsorption on ferrihydrite: kinetics, equilibrium and adsorption envelops. Environ Sci Technol 1998;32:344–9.